







# Ceragenins and Antimicrobial Peptides Kill Bacteria through Distinct Mechanisms

 Gabriel Mitchell,<sup>a\*</sup> Melanie R. Silvis,<sup>b</sup> Kelsey C. Talkington,<sup>a</sup> Jonathan M. Budzik,<sup>a,c</sup> Claire E. Dodd,<sup>a</sup> Justin M. Paluba,<sup>a</sup> Erika A. Oki,<sup>a</sup> Kristine L. Trotta,<sup>d</sup> Daniel J. Licht,<sup>a</sup>  David Jimenez-Morales,<sup>e,f</sup> Seemay Chou,<sup>d,k</sup> Paul B. Savage,<sup>g</sup> Carol A. Gross,<sup>b,h</sup>  Michael A. Marletta,<sup>a,i,j</sup>  Jeffery S. Cox<sup>a</sup>

<sup>a</sup>Department of Molecular and Cell Biology, University of California, Berkeley, California, USA

<sup>b</sup>Department of Microbiology and Immunology, University of California, San Francisco, California, USA

<sup>c</sup>Department of Medicine, University of California, San Francisco, California, USA

<sup>d</sup>Department of Biochemistry and Biophysics, University of California, San Francisco, California, USA

<sup>e</sup>Department of Medicine, Division of Cardiovascular Medicine, Stanford University, California, USA

<sup>f</sup>Department of Cellular and Molecular Pharmacology, University of California, San Francisco, California, USA

<sup>g</sup>Department of Chemistry and Biochemistry, Brigham Young University, Provo, Utah, USA

<sup>h</sup>Department of Cell and Tissue Biology, University of California, San Francisco, California, USA

<sup>i</sup>Department of Chemistry, University of California, Berkeley, California, USA

<sup>j</sup>California Institute for Quantitative Biosciences, University of California, Berkeley, California, USA

<sup>k</sup>Chan Zuckerberg Biohub, San Francisco, California, USA

**ABSTRACT** Ceragenins are a family of synthetic amphipathic molecules designed to mimic the properties of naturally occurring cationic antimicrobial peptides (CAMPs). Although ceragenins have potent antimicrobial activity, whether their mode of action is similar to that of CAMPs has remained elusive. Here, we reported the results of a comparative study of the bacterial responses to two well-studied CAMPs, LL37 and colistin, and two ceragenins with related structures, CSA13 and CSA131. Using transcriptomic and proteomic analyses, we found that *Escherichia coli* responded similarly to both CAMPs and ceragenins by inducing a Cpx envelope stress response. However, whereas *E. coli* exposed to CAMPs increased expression of genes involved in colanic acid biosynthesis, bacteria exposed to ceragenins specifically modulated functions related to phosphate transport, indicating distinct mechanisms of action between these two classes of molecules. Although traditional genetic approaches failed to identify genes that confer high-level resistance to ceragenins, using a Clustered Regularly Interspaced Short Palindromic Repeats interference (CRISPRi) approach we identified *E. coli* essential genes that when knocked down modify sensitivity to these molecules. Comparison of the essential gene-antibiotic interactions for each of the CAMPs and ceragenins identified both overlapping and distinct dependencies for their antimicrobial activities. Overall, this study indicated that, while some bacterial responses to ceragenins overlap those induced by naturally occurring CAMPs, these synthetic molecules target the bacterial envelope using a distinctive mode of action.

**IMPORTANCE** The development of novel antibiotics is essential because the current arsenal of antimicrobials will soon be ineffective due to the widespread occurrence of antibiotic resistance. The development of naturally occurring cationic antimicrobial peptides (CAMPs) for therapeutics to combat antibiotic resistance has been hampered by high production costs and protease sensitivity, among other factors. The ceragenins are a family of synthetic CAMP mimics that kill a broad spectrum of bacterial species but are less expensive to produce, resistant to proteolytic degradation, and seemingly resistant to the development of high-level resistance. Determining how ceragenins function may identify new essential biological pathways of bacteria that are less prone to the development of resistance and will further our understanding of the design principles for maximizing the effects of synthetic CAMPs.

**Editor** Gerard D. Wright, McMaster University

**Copyright** © 2022 Mitchell et al. This is an open-access article distributed under the terms of the [Creative Commons Attribution 4.0 International license](https://creativecommons.org/licenses/by/4.0/).

Address correspondence to Michael A. Marletta, marletta@berkeley.edu, or Jeffery S. Cox, jeff.cox@berkeley.edu.

\*Present address: Gabriel Mitchell, Open Innovation at Novartis Institute for Tropical Diseases, Emeryville, California, USA.

The authors declare no conflict of interest.

**Received** 13 September 2021

**Accepted** 21 December 2021

**Published** 25 January 2022

**KEYWORDS** Antibiotics, Gram-negative, Gram-positive, mycobacteria, CSA

Our current arsenal of antibiotics will soon be ineffective against the simplest bacterial infections due to the continued spread of antibiotic resistance (AR) (1). AR has been identified in virtually all bacterial species of clinical relevance, including Gram-positive and Gram-negative bacteria as well as mycobacteria (2). Despite the threat that AR represents to global health, there is a lack in the development of antimicrobials with innovative mechanisms of action (3–5). A better understanding of the fundamental principles of how antibiotics kill microbes and how AR develops is key to breaking the futile cycle of antibiotic development and microbial evolution.

Antimicrobial peptides are structurally diverse molecules expressed in a wide array of organisms that directly kill microbes, including bacteria (6, 7). Many antimicrobial peptides, such as the class of cationic antimicrobial peptides (CAMP), rapidly kill bacteria likely by disrupting membranes, although other mechanisms of action have been suggested (7–9). The potential of using CAMPs to treat AR infections has become a research focus due to their action against a broad spectrum of pathogens, their selectivity toward microbial membranes, and the slow development of resistance (6, 10). Despite some progress in this area, significant barriers to CAMP therapeutic development include high production costs, toxicity, susceptibility to proteolytic degradation, and activation of allergic responses (6, 10).

Ceragenins are a family of synthetic amphipathic molecules derived from cholic acid designed to mimic the activity of endogenous CAMPs (11, 12). These molecules are inexpensive to manufacture and are not susceptible to proteolysis, making them an attractive alternative to peptide-based synthetic CAMPs (11). Importantly, ceragenins have antimicrobial activity against a broad spectrum of microbes, which include both Gram-negative and Gram-positive bacteria (11). High-level resistance to ceragenins is seemingly difficult to acquire in the lab as attempts to isolate ceragenin-resistance bacterial mutants failed in the Gram-positive bacterium *Staphylococcus aureus* and identified only modest and unstable resistance in Gram-negative organisms (13). Although ceragenins were designed as CAMP mimics and can depolarize bacterial membranes (14), the inability to identify bonafide ceragenin-resistant bacterial mutants represents a major barrier in understanding their mechanism of action.

Here, we took a comparative strategy and used a combination of transcriptomic, proteomic, and genetic approaches to study the bacterial responses to treatment with ceragenins and two well-studied CAMPs. The results of this study suggested that ceragenins kill bacteria by disrupting the bacterial envelope through a distinctive mode of action from naturally occurring CAMPs. We also showed that ceragenins have activity against mycobacteria despite their unique cell wall architecture.

## RESULTS

**Susceptibility of bacteria to CAMPs and ceragenins.** MICs for the CAMPs colistin and LL37 as well as two ceragenin compounds, CSA13 and CSA131 (see structures in Fig. 1A), were determined against the Gram-negative bacterium *E. coli*, the Gram-positive bacterium *Listeria monocytogenes* and several mycobacterial species (i.e., *Mycobacterium avium*, *M. marinum*, *M. smegmatis*, and *M. tuberculosis*) (Fig. 1B to H and Table S1). *M. avium* mc<sup>2</sup>2500 and mc<sup>2</sup>2500D are two colony morphotypes of a clinical strain that predominantly form either smooth/transparent (mc<sup>2</sup>2500) or opaque (mc<sup>2</sup>2500D) colonies (15). The fluoroquinolone antibiotic ciprofloxacin (CIP), which inhibits DNA gyrase, was included as a positive-control. As expected, colistin, which requires binding to lipopolysaccharide (LPS) for activity (16), was active against *E. coli* (Fig. 1B) but not against *L. monocytogenes* (Fig. 1C) or any of the mycobacterial species (Fig. 1D to H). Interestingly, LL37 was active against *E. coli* (Fig. 1B) and *L. monocytogenes* (Fig. 1C) but had no detectable activity against mycobacterial species (Fig. 1D to H). The ceragenins CSA13 and CSA131 were also active against both *E. coli* (Fig. 1B) and *L. monocytogenes* (Fig. 1C). In contrast to colistin and LL37, the ceragenins had activity against mycobacteria, although the MICs varied between species (Fig. 1D to H). While *M. smegmatis* was highly susceptible to CSA13 and CSA131 (Fig. 1G), both compounds were less active against

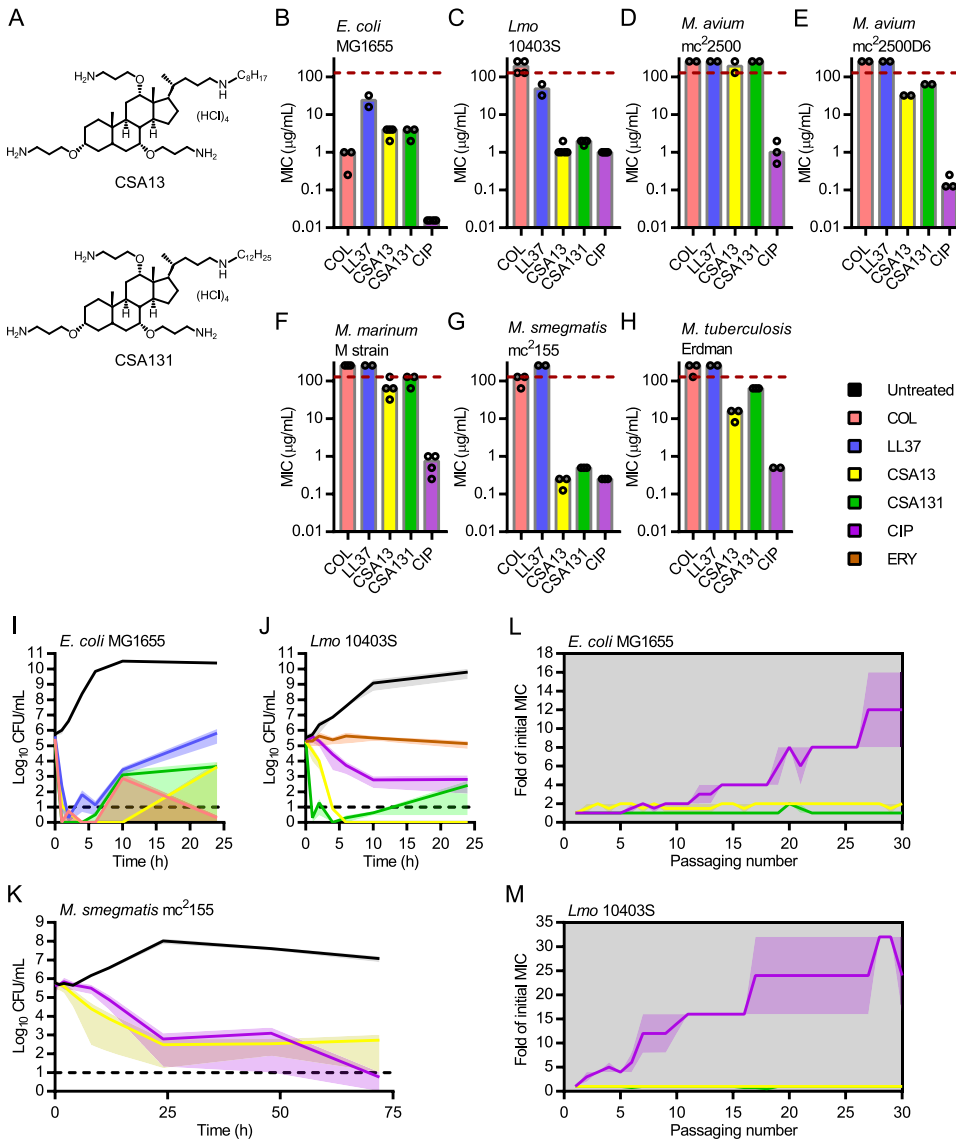


**FIG 1** Ceragenins kill phylogenetically diverse bacteria. (A) Structures of the ceragenins CSA13 and CSA131. MICs of colistin (COL), LL37, CSA13, CSA131, and ciprofloxacin (CIP) against *E. coli* MG1655 (B), *L. monocytogenes* (*Lmo*) 10403S (C), *M. avium* mc<sup>2</sup>2500 (D), *M. avium* mc<sup>2</sup>2500D6 (E), *M. marinum* M strain (F), *M. smegmatis* mc<sup>2</sup>155 (G) and *M. tuberculosis* Erdman (H). Dots and bars indicate results from independent experiments and median values, respectively. Time-kill experiments of *E. coli* MG1655 (I), *L. monocytogenes* 10403S (J), and *M. smegmatis* mc<sup>2</sup>155 (K) exposed to colistin (in pink), LL37 (in blue), CSA13 (in yellow), CSA131 (in green), ciprofloxacin (in purple) and/or erythromycin (ERY; in orange), a bacteriostatic antibiotic. Untreated samples are in black, and results are shown as means from two independent experiments. Shaded areas show standard error of the mean (SEM), and dotted lines indicate the limit of detection. Serial passages of *E. coli* (L) and *L. monocytogenes* (M) exposed to CSA13 (in yellow), CSA131 (in green), and ciprofloxacin (in purple). Bacteria were passaged daily in the presence of subinhibitory concentrations of antibiotics. Results are expressed as means and SEM from two independent experiments.

the slower-growing species *M. avium* (Fig. 1D and E), *M. marinum* (Fig. 1F), and *M. tuberculosis* (Fig. 1H). Similar trends in MIC values for *E. coli*, *L. monocytogenes*, and *M. smegmatis* were observed with two other structurally related ceragenin compounds, CSA44 and CSA144 (See Table S1), which further confirmed that ceragenins have antimicrobial activity against mycobacteria. Overall, these results demonstrate that the spectrum of activity of ceragenins is broader than colistin and LL37, indicating different requirements for activity.

**Ceragenins are bactericidal.** To determine if ceragenins kill all three types of bacteria, we performed survival experiments at inhibitory concentrations (~1 to 2 × MICs) of the molecules (Fig. 1I to K). Like colistin, LL37 and ciprofloxacin, ceragenin treatment (CSA13 or

CSA131) led to cell killing of *E. coli* (Fig. 1I), *L. monocytogenes* (Fig. 1J), and *M. smegmatis* (Fig. 1K), although some bacteria began to grow slightly by the end of the culturing, perhaps due to inactivation of the antibiotic or the emergence of resistant bacteria at these later time points. This late regrowth phenotype seemed to be highly dependent on antibiotic concentration and was not observed in a *L. monocytogenes* culture treated with a 2-fold higher concentration (4  $\mu\text{g}/\text{mL}$ ) of CSA131 (data not shown). The bactericidal activities of CAMPs, ceragenins, and ciprofloxacin are in contrast with the activity of the bacteriostatic antibiotic erythromycin against *L. monocytogenes* (Fig. 1J), which did not cause any significant reduction in cell number but inhibited bacterial growth. Overall, these results confirmed that ceragenins act on bacteria through a bactericidal mechanism.

**Serial passage of *E. coli* and *L. monocytogenes* in the presence of subinhibitory concentrations of ceragenins.** Isolation and characterization of antibiotic-resistant bacteria could provide insight into the mode of action of ceragenins. Although a previous study showed that bacterial resistance to ceragenins is infrequently observed *in vitro* and unstable (13), the late regrowth of bacteria that was observed when they were exposed to ceragenins during the previous survival experiments (Fig. 1I and J) led us to attempt generating ceragenin-resistant bacteria. To this end, we performed serial passaging experiments with *E. coli* and *L. monocytogenes* in the presence of ciprofloxacin, CSA13, and CSA131 (Fig. 1L and M). During these experiments, bacteria were cultured overnight in the presence of a range of antimicrobial concentrations, and bacteria that grew at the highest concentration of antimicrobials (right below MIC) were used as inoculums for the next growth cycle. A total of 30 passages were performed for both bacterial species, and antibiotic susceptibilities were determined and recorded for each of these passages to monitor the gradual emergence of resistance to the antimicrobials. In contrast to ciprofloxacin-exposed bacteria, *E. coli* and *L. monocytogenes* bacteria exposed to ceragenins did not give rise to stable resistance (Fig. 1L and M). The generation of spontaneous *M. smegmatis* mutants resistant to CSA13 was also attempted, but no CSA13-resistant bacteria were recovered, although bacteria resistant to ciprofloxacin and rifampicin were isolated from parallel control experiments (data not shown). These results confirmed that resistance to ceragenins is infrequent (13) and does not emerge *in vitro* under conditions known to generate resistant mutants against other antibiotics.

**Transcriptional response of *E. coli* exposed to ceragenins.** To gain insights into the mechanism of action of CAMPs and ceragenins, we determined the global transcriptional responses of *E. coli* exposed to colistin, LL37, CSA13, and CSA131 using RNAseq, as similarly used for other antibacterial compounds (17, 18). Bacteria were grown to log phase and then treated with supra-MICs of antibiotics for 1 h before RNA extraction and sequencing (see Materials and Methods). Plots of the normalized number of reads per gene showed excellent correlation ( $R = 0.965$  to  $0.999$ ) between biological replicates for each of the conditions tested (Fig. 2A to D), demonstrating the reproducibility of the method. Hundreds of statistically significant changes in gene expression (defined by absolute  $\log_2$ -fold change  $>1$  and adjusted  $P$  value  $<0.05$ ) following exposure of bacteria to colistin, LL37, CSA13, and CSA131 were measured (Fig. 2E to H and Data Set S1).

The global transcriptional responses of *E. coli* to CAMPs and ceragenins were analyzed using multidimensional scaling analysis. Interestingly, while transcriptional responses of bacteria to the CAMPs colistin and LL37 were essentially the same, the response to CSA13 and CSA131 were not only distinct from these CAMPs but also distinct from each other (Fig. 2I). Pathway analysis corroborated that *E. coli* responded differently to CAMPs and ceragenins and showed enrichment of annotation terms associated with the outer membrane (e.g., lipopolysaccharide and colanic acid) in genes upregulated by CAMPs but not ceragenins (Fig. 2J and Data set S2). Pathway analysis also corroborated the heterogeneity in the bacterial response to ceragenins and showed enrichment of terms associated with translation in genes downregulated by CSA13 but not CSA131 (Fig. 2K and Data Set S2). While the two ceragenins are structurally quite similar, the addition of four methylene groups to the CSA13 carbon chain to

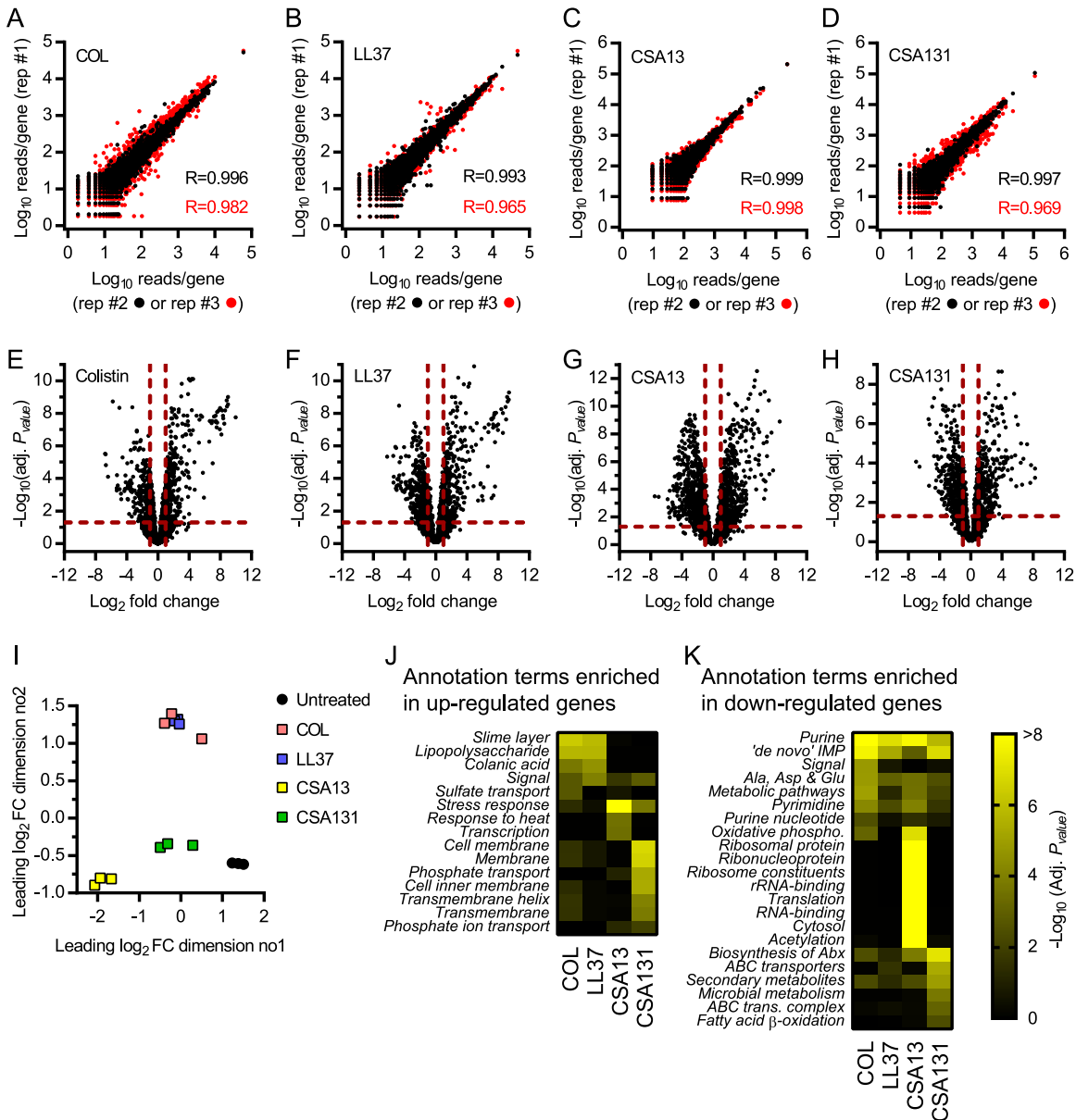


**FIG 2** Transcriptional response of *E. coli* exposed to ceragenins. RNA from exponentially growing *E. coli* bacteria exposed to supra-MICs of colistin (COL), LL37, CSA13, and CSA131 was extracted and sequenced. (A–D) Replica plots showing the  $\log_{10}$  of the normalized number of reads per gene for bacteria exposed to antibiotics. Correlation coefficients ( $R$ ) between replicates #1 and #2 (black dot) and #1 and #3 (red dot) are displayed. (E–H) Volcano plots that represent RNA expression as means of  $\log_2$ -fold change and  $-\log_{10}$  adjusted  $P$  values (adj.  $P$  value) for bacteria exposed to antibiotics in comparison to untreated control samples. Horizontal and vertical dotted red lines indicate adjusted  $P$  values less than 0.05 (or  $-\log_{10}$  [adj.  $P$  value] greater than 1.3) and absolute  $\log_2$ -fold change greater than 1. (I) Multidimensional scaling (MDS) plot showing the separation between biological replicates and between untreated and antibiotic-treated samples. (J) Annotation terms enriched for genes significantly upregulated ( $\log_2$  FC > 1 and adj.  $P$  value < 0.05) following exposure to antibiotics. (K) Annotation terms enriched for genes significantly downregulated ( $\log_2$  FC < -1 and adj.  $P$  value < 0.05) following exposure to antibiotics. Adjusted  $P$  values of annotation terms associated with a false discovery rate (FDR) value > 0.05 for at least one antibiotic are shown. Only the 8 most statistically significant annotation terms are shown for each condition. Annotation terms are abbreviated and/or modified for a purpose of presentation (see Data Set S2 for original annotation terms). Data are from 3 independent experiments.

create CSA131 significantly alters the hydrophobicity of the molecule, increasing the partition coefficient from  $\log P_{\text{CSA13}} = 5.51$  to  $\log P_{\text{CSA131}} = 7.29$  (see Materials and Methods), which likely contributes to differences in antibacterial activities and bacterial responses. Overall, these results showed that transcriptional responses of *E. coli* to the naturally occurring CAMPs colistin and LL37 are similar but differ from the response to ceragenins, identifying for the first time that these CAMP mimics have a distinct

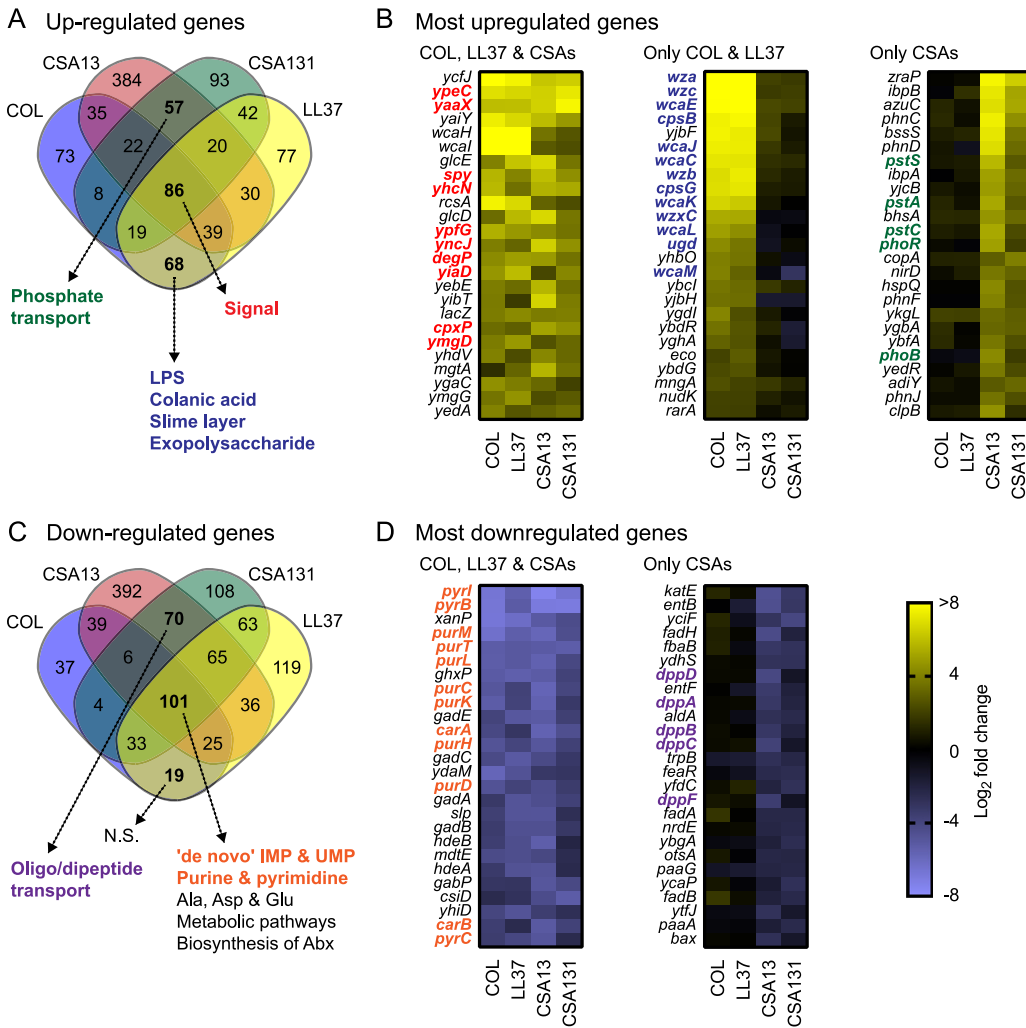


**FIG 3** Identification of pathways defining the transcriptional response of *E. coli* to ceragenins. (A) Venn diagram analysis of genes significantly upregulated ( $\log_2$  FC >1 and adjusted *P* value <0.05) in *E. coli* exposed to antibiotics. Annotation terms associated with a false discovery rate (FDR) value > 0.05 for genes upregulated by all antibiotics, by CAMPs, or by ceragenins are shown by dotted arrows. (B) Top 25 most upregulated genes for bacteria exposed to all antibiotics (COL, LL37 & CSAs), CAMPs (COL & CSAs), or ceragenins. Genes belonging to the annotation terms signal (in red), LPS, colanic acid, slime layer, and exopolysaccharide (in blue), and phosphate transport (in green) are indicated. (C) Venn diagram analysis of genes significantly downregulated ( $\log_2$  FC <-1 and adjusted *P* value <0.05) in *E. coli* exposed to antibiotics. Annotation terms associated with a false discovery rate (FDR) value > 0.05 for genes downregulated by all antibiotics, by CAMPs, or by ceragenins are shown by dotted arrows. (D) Top 25 most downregulated genes for bacteria exposed to all antibiotics or ceragenins. Genes belonging to the annotation terms “*de novo* IMP”, “*de novo* UMP”, “purine”, and “pyrimidine” (in orange), and “oligonucleotide/dipeptide transport” (in purple) are indicated. Annotation terms are abbreviated and/or modified for a purpose of presentation (see Data Set S3 for original annotation terms). Data are from 3 independent experiments.

function. These results also suggested that *E. coli* responds differently to the structurally related ceragenin compounds, CSA13 and CSA131.

**Identification of pathways defining the transcriptional response of *E. coli* to ceragenins.** Pathway analysis of genes modulated by more than one compound was performed to further define transcriptional responses to CAMPs and ceragenins. The Venn diagram in Fig. 3A visualizes the extent of overlap of the individual *E. coli* genes that had significant increases in mRNA abundance upon treatment with each of the molecules. In particular, 86 genes were induced in all 4 conditions, 68 were upregulated specifically during CAMP treatment while 57 were induced by the ceragenins (Fig. 3A and Data Set S3). The annotation term “signal” was significantly enriched among the genes upregulated by all antibiotics (Fig. 3A and Data Set S3), which is indicative of a common response to CAMPs and ceragenins. Interestingly, this group included genes involved in the membrane stress response such as *spy*, *degP*, and *cpxP* (19) (Fig. 3B). Consistent with results from Fig. 2, genes

specifically upregulated in bacteria exposed to CAMPs were significantly associated with annotation terms related to LPS/colanic acid biosynthesis and included genes such as *wzc*, *wcaE*, and *cpsB* (Fig. 3A and B and Data Set S3). Interestingly, genes specifically upregulated in bacteria exposed to ceragenins were associated with phosphate transport (Fig. 2J, Fig. 3A, and Data Set S3) and included genes encoding the major phosphate-responsive regulators PhoR and PhoB (Fig. 3B). Overall, these results suggested that *E. coli* responds to CAMPs and ceragenins by upregulating genes involved in signaling and the response to membrane stress. These results also showed that, while exposure of *E. coli* to CAMPs specifically induces the expression of genes related to LPS and colanic acid biosynthesis, exposure to ceragenins uniquely induces the expression of genes involved in phosphate transport.

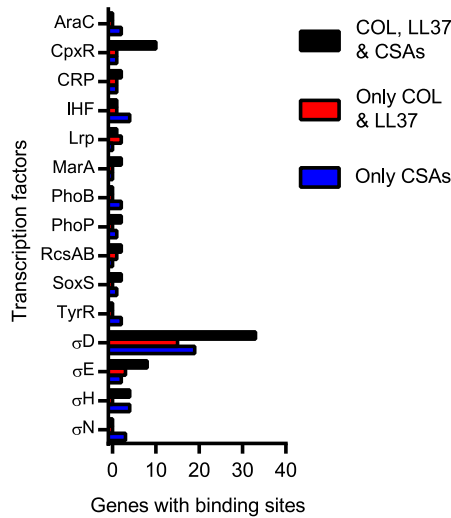
For genes with mRNA levels that decreased during these treatments, 101 were downregulated by all antibiotics, 19 by CAMPs, and 70 by ceragenins (Fig. 3C and Data Set S3). Pathway analysis identified significant enrichment of terms related to amino acids and nucleotide metabolism in genes downregulated following exposure to all antibiotics (Fig. 3C and Data Set S3). This was corroborated by the finding that genes related to purine and pyrimidine biosynthesis (e.g., *pyrB*, *purM*, and *purT*) were among the most significantly downregulated genes by these antimicrobials (Fig. 3D), which is consistent with our pathway analysis (Fig. 2K). Genes downregulated by ceragenins showed enrichment for genes involved in oligopeptide/dipeptide transport such as *dppD* and *dppA* (Fig. 3C, Fig. 3D, and Data Set S3). Although the reason for the downregulation of genes involved in peptide transport in *E. coli* exposed to ceragenins is unknown, these results suggested that bacteria exposed to CAMPs and ceragenins respond by downregulating genes involved in metabolic pathways.

**Identification of cis-acting elements that regulate the transcriptional response of *E. coli* to ceragenins.** To determine which signal transduction pathways control the transcriptional responses to CAMPs and ceragenins, the DNA sequences immediately 5' of genes with significantly altered mRNA levels were analyzed for the presence of cis-acting promoter and operator sequences known or predicted to bind transcriptional regulators (20). Interestingly, genes upregulated following exposure to each of the molecules (Fig. 4A and Data Set S4) were associated with cis-acting elements that interact with the response regulator CpxR of the CpxA/CpxR two-component regulatory system (enrichment of 11.63%; 10 out of 86 genes), which responds to the envelope stress (21) and is consistent with the upregulation of the CpxR regulon genes *spy*, *degP* and *cpxP* (Fig. 3B). This analysis also showed enrichment for genes associated with cis-acting elements binding the primary sigma factor  $\sigma^D$  (22), involved in the redistribution of the RNA polymerase in response to osmotic stress (23), the alternative sigma factor  $\sigma^E$  that coordinates the envelope stress response (21, 24, 25), and the alternative sigma factor  $\sigma^{H1}$ , which controls the expression of heat shock genes and genes involved in membrane functionality and homeostasis (26) (Fig. 4A). Genes downregulated following exposure to all antibiotics were associated with the presence of binding sites for the HTH-type transcriptional repressor PurR (Fig. 4B and Data Set S4), which regulates genes involved in the *de novo* synthesis of purine and pyrimidine nucleotides (27, 28), and corroborated our analysis above (Fig. 2K, and 3C and D). Overall, these results suggested that CAMPs and ceragenins perturb the bacterial envelope and trigger the CpxA/CpxR system. These results also suggested that PurR downregulates the expression of genes involved in the biosynthesis of purine and pyrimidine following the exposure of *E. coli* to CAMPs and ceragenins.

**Expression of the CpxR, PurR, RcsA, and PhoB regulons in *E. coli* exposed to ceragenins.** To further confirm a role for CpxR and PurR in the response of *E. coli* to CAMPs and ceragenins, the expression of the CpxR and PurR regulons was analyzed in more detail (Fig. 5A and B and Data Set S4). The heat map of the CpxR regulon showed a consistent regulation of several genes in bacteria exposed to all four compounds (e.g., *cpxP*, *degP*, *dsbA*, *spy*, and *yebE*) (Fig. 5A) and corroborated our results described above (Fig. 3B and 4A). Likewise, most of the genes of the PurR regulon were also downregulated under these conditions (Fig. 5B), again consistent with our findings described above (Fig. 2K, 3C and D, and 4B). These results confirmed that the expression of the CpxR and PurR regulons are modulated in *E. coli* exposed to CAMPs and ceragenins.

Our expression analysis led us to focus on the RcsA and PhoB regulons to gain

**A Up-regulated genes**



**B Down-regulated genes**

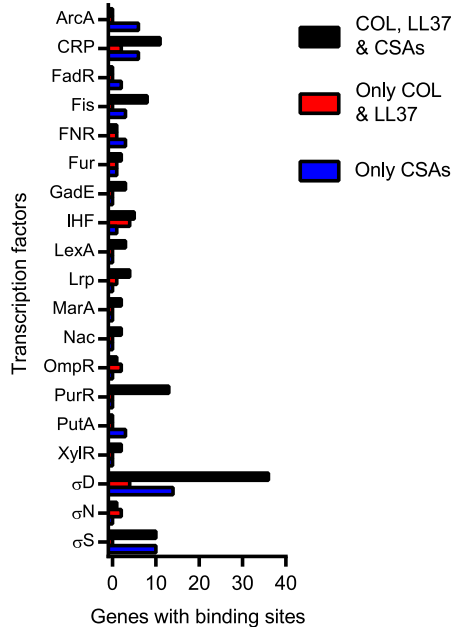


**FIG 4** Identification of cis-acting elements that regulate the transcriptional response of *E. coli* to ceragenins. Genes with known or predicted promoters or binding sites for transcription factors are enumerated for genes commonly upregulated (A) or downregulated (B) by all antibiotics (black bars), by CAMPs (red bars), or by ceragenins (in blue). Only promoters and binding sites identified more than once for at least one group are represented.

insight into the differential regulation of genes involved in the biosynthesis of colanic acid and phosphate transport, respectively (Fig. 5C and D and Data Set S4). RcsA regulates the expression of genes involved in colanic acid biosynthesis (21), a pathway that was upregulated in *E. coli* exposed to CAMPs, but not ceragenins (Fig. 2J, and 3A and B). Accordingly, the heat map of the RcsA regulon showed a marked modulation of this pathway in *E. coli* exposed to CAMPs in comparison to ceragenins (Fig. 5C). The phosphate regulon transcriptional regulatory protein PhoB regulates the expression of genes involved in phosphate transport (29) and was upregulated in *E. coli* following exposure to ceragenins, but not CAMPs (Fig. 2J, and 3A and B). Accordingly, the heat map of the PhoB regulon showed partial but specific induction in bacteria exposed to ceragenins (Fig. 5D). More specifically, upregulation of the *phnC-phnP*



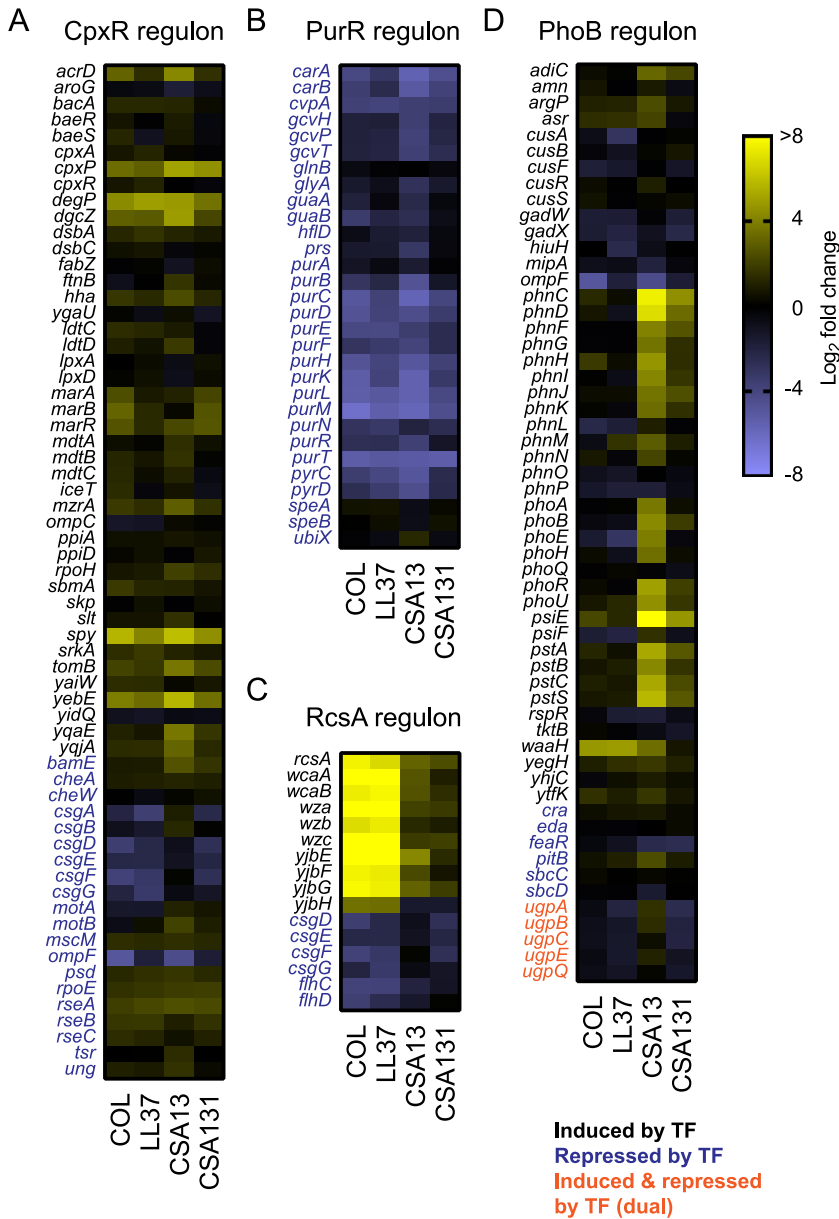


**FIG 5** Expression of the CpxR, PurR, RcsA, and PhoB regulons in *E. coli* exposed to ceragenins. Heat maps of log<sub>2</sub>-fold change for genes of the CpxR (A), PurR (B), RcsA (C), and PhoB (D) regulons in bacteria exposed to antibiotics. Genes predicted to be induced (in black), repressed (in blue) or both (in orange) by specific transcription factors are indicated. Data are from 3 independent experiments.

operon, the *pstSCAB-phoU* operon as well as a trend for other *pho* genes (e.g., *phoB* and *phoR*) and the phosphate starvation-inducible *psiEF* genes were specifically observed in bacteria exposed to ceragenins (Fig. 5D). These results suggested that the specific upregulation of genes involved in colanic acid biosynthesis and phosphate transport in bacteria exposed to CAMPs and ceragenins are mediated by RcsA and PhoB, respectively.

**Proteomic response of *E. coli* exposed to colistin and CSA13.** To validate the previous conclusions as well as to determine if the changes in mRNA levels in response to the molecules led to changes in the proteome, we measured global protein abundance in bacteria exposed to colistin and CSA13 by mass spectrometry-based proteomics. *E. coli* cultures were grown to log phase and treated with supra-MICs of antibiotics before protein extraction, peptide preparation, and peptide quantification (see Materials and Methods). Approximately 1800 unique proteins were detected for each biological replicate (Fig. 6A) and the number of unique peptides identified showed an excellent correlation

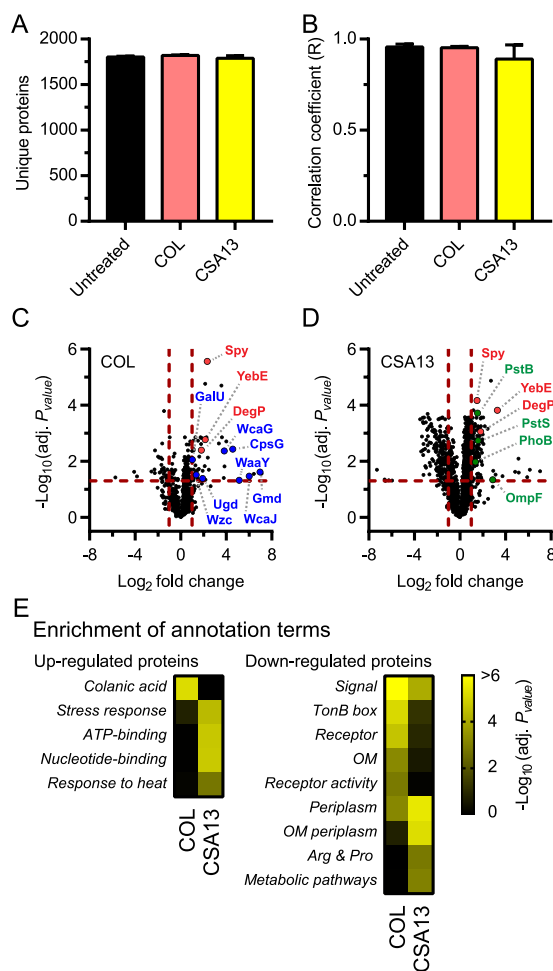


**FIG 6** Proteomic response of *E. coli* exposed to colistin and CSA13. (A) The number of unique proteins identified for each condition. (B) Correlation coefficient (R) for the number of peptides per protein between the biological replicates of untreated bacteria and bacteria exposed to colistin (COL) or CSA13. Data are represented as means and standard deviations. (C and D) Volcano plots that represent protein expression as means of  $\log_2$ -fold change and  $-\log_{10}$  adjusted *P* values (adj. *P* value) for bacteria exposed to antibiotics in comparison to untreated controls. Horizontal and vertical dotted red lines indicate adjusted *P* values less than 0.05 (or  $-\log_{10}$  [adj. *P* value] greater than 1.3) and absolute  $\log_2$ -fold change greater than 1. Some upregulated proteins that are members of the Cpx regulon (in red), involved in colanic acid and LPS biosynthesis (in blue), or members of the PhoB regulon (in green) are highlighted. (E) Annotation terms enriched for proteins significantly up- or downregulated (absolute  $\log_2$  FC >1 and adj. *P* value <0.05) following the exposure of *E. coli* to colistin and CSA13. Adjusted *P* values of annotation terms associated with a false discovery rate (FDR) value >0.05 for at least one antibiotic are shown. Annotation terms are abbreviated and/or modified for a purpose of presentation (see Data Set S6 for original annotation terms). Data are from 3 independent bacterial cultures for each condition.

between biological replicates (Fig. 6B). Several statistically significant changes in protein expression (absolute  $\log_2$ -fold change >1 and adjusted *P* value <0.05) were observed following exposure of *E. coli* to colistin (Fig. 6C) and CSA13 (Fig. 6D) (see Data Set S5). This dataset showed that *E. coli* exposed to both colistin and CSA13 upregulated the proteins DegP, Spy, and YebE (Fig. 6C and D, and Table S2), which are known members of the Cpx regulon (19) that were strongly upregulated at the transcriptional level following exposure to CAMPs and ceragenins (Fig. 5A and Table S2). The dataset also revealed modulation of proteins involved in colanic acid and LPS biosynthesis (e.g., Ugd and WcaG) (Fig. 6C and Table S2) or related to the PhoB regulon (e.g., PstB and PstS) (Fig. 6D and Table S2) in bacteria exposed to colistin or CSA13, respectively, which also corroborate our transcriptional data (Fig. 5C and D, and Table S2). Therefore, the proteomic data are consistent with our transcriptional analysis and revealed a common induction of the Cpx envelope stress

response in response to CAMPs and ceragenins. The results also corroborated that colistin and CSA13 specifically induced proteins involved in colanic acid biosynthesis and modulated members of the PhoB regulon, respectively.

Annotation term enrichment analysis was performed on the proteomic dataset to identify pathways significantly modulated in bacteria exposed to colistin and CSA13 (see Data Set S6). Similar to our transcriptional results (Fig. 2J), the colanic acid pathway was significantly enriched among proteins upregulated by colistin but not CSA13 (Fig. 6E). A heat response signature was significantly enriched among proteins upregulated by CSA13 but not colistin (Fig. 6E), corroborating the transcriptional upregulation of genes associated with this pathway and with *cis*-acting elements for  $\sigma^H$  (Fig. 2J and 4A, and Table S2). In addition, while the periplasm pathway was enriched among proteins downregulated by both colistin and CSA13, the outer membrane pathway was significantly enriched among proteins downregulated by colistin but not by CSA13 (Fig. 6E). Overall, these results confirmed that *E. coli* responded distinctly to colistin and CSA13, although both compounds modulated proteins associated with the bacterial envelope. Thus, while both molecules triggered a common set of genes involved in bacterial envelope stress, they also activated distinct response pathways, indicating they have overlapping but not identical modes of action.

**Identification of genetic determinants of resistance to ceragenins in *E. coli*.** Our inability to identify ceragenin-resistant *E. coli* mutants (Fig. 1L and M) was consistent with results previously published by Pollard et al. (13) and indicated that resistance to ceragenins emerged infrequently in culture despite strong selective pressure. This suggested that ceragenins either have multiple essential targets or affect cellular structures that are immutable. Thus, traditional genetic approaches to identify the target(s) of ceragenins have not been feasible. To gain insight into the genetic determinants of ceragenin action, we employed an alternative genetic approach that utilizes CRISPRi to reduce the expression of genes in *E. coli*. As demonstrated previously, this approach allows for partial knockdown of essential *E. coli* genes, practically creating hypomorphic alleles that have reduced function but still promote cell viability (30, 31). By combining these genetic perturbations with subinhibitory concentrations of antibiotics and by measuring the effects on bacterial fitness, we sought to identify functional interactions between bacterial pathways and antibiotic stress.

We screened a pooled library of inducible knockdown strains targeting essential genes (30) grown with or without subinhibitory concentrations of CAMPs or ceragenins. To evaluate the fitness of each CRISPRi knockdown within the complex population, we used deep sequencing to measure the relative abundance of guide sequences during the different culturing conditions.  $\log_2$ -fold changes ( $\log_2$  FC) in abundance in response to CAMPs and ceragenins were calculated in comparison to the control condition for each knockdown strain, and significantly resistant or sensitized strains (defined by absolute  $\log_2$ -fold change  $> 0.5$  and an adjusted *P* value  $< 0.05$ ) were identified for each of the compounds (Fig. 7A to D and Data Set S7). Although no clear correlation was observed between hits identified using the CRISPRi approach and the transcriptional responses analyzed above (Table S3), CRISPRi strains depleted or enriched following exposure to one or several antimicrobials were predominantly knocked down for genes involved in the bacterial envelope. This provided further evidence that the bacterial envelope is the cellular structure targeted by both CAMPs and ceragenins.

The changes in abundance for the genes identified above were further analyzed and compared between treatments (Fig. 7E). Several genes involved in the LPS biosynthetic pathway were identified in these screens, and knockdown of the lipid-A-disaccharide synthase LpxB (32) sensitized *E. coli* to all the compounds, highlighting the bacterial surface as a common site of action for CAMPs and ceragenins. Silencing of the LPS transport genes *lptB* and *lptF* (33) led to sensitivity to colistin, LL37, and CSA131 but not to CSA13, which corroborates the above transcriptomic data and suggests distinctive mechanisms of action for CSA13 and CSA131 (Fig. 2I to K). Knockdown of *kdsC* (34), encoding an enzyme involved in LPS biosynthesis, only led to sensitivity to LL37. Knockdown strains for *rpoE*, the gene encoding the envelope stress-responsive sigma factor  $\sigma^E$  (21, 24, 25), and the ubiquinone biosynthesis gene *ubiJ* (35) were sensitive to CSA13 but not to CSA131, which also supports the idea that these ceragenins act distinctively on bacteria. On the other hand, the knockdown

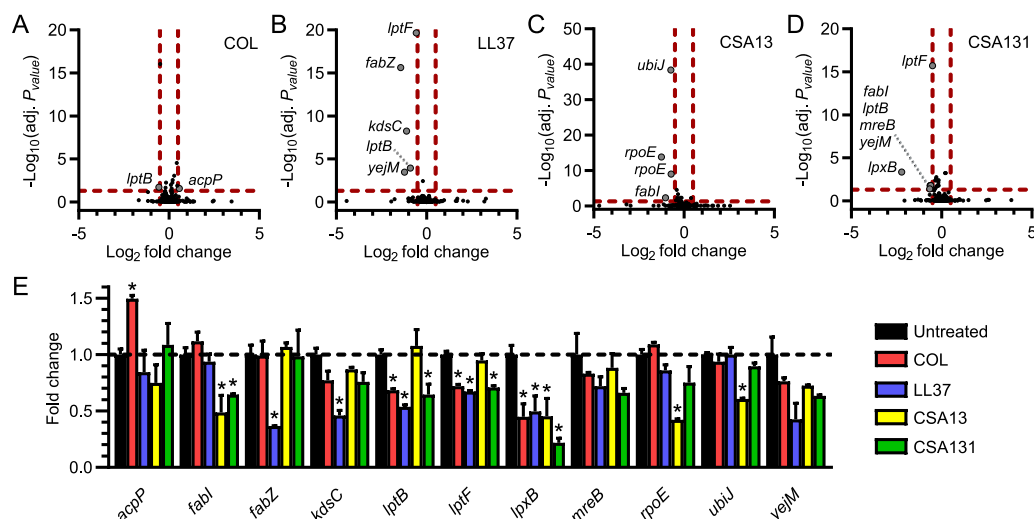


**FIG 7** Identification of the genetic determinants of resistance to ceragenins in *E. coli* using CRISPRi. A pooled CRISPRi library that allows the inducible knockdown of predicted essential genes was used to study the genetic determinants of resistance to CAMPs and ceragenins. Changes in abundance (Log<sub>2</sub>FC) and adjusted *P* values ( $-\log_{10}$  [adj. *P* value]) associated with each strain following exposure to colistin (COL) (A), LL37 (B), CSA13 (C), and CSA131 (D) are shown. Horizontal and vertical dotted red lines indicate adjusted *P* values less than 0.05 (or  $-\log_{10}$  [adj. *P* value] greater than 1.3) and absolute log<sub>2</sub>-fold change greater than 0.5. Genes associated with significant changes in abundance are labeled for each compound. (E) Mean fold changes in abundance and standard deviations (SD) associated with significantly enriched or depleted CRISPRi strains (only one *rpoE*-targeting strain is shown) following exposure to COL, LL37, CSA13, and CSA131 (\*, *P* < 0.05 [two-tailed unpaired *t* test]). Means and SDs were calculated from counts normalized to the total number of counts for each condition. Data are from two biological replicates.

strain for the fatty acid biosynthesis gene *fabI* (36, 37) was sensitive to both CSA13 and CSA131 and not to the CAMPs and may constitute a common molecular determinant of sensitivity to ceragenins. Other genes involved in fatty acid metabolism were identified as genetic interactors with CAMPs. More specifically, interference with the expression of *acpP*, encoding the acyl carrier protein (38), led to resistance to colistin, whereas knockdown of *fabZ*, encoding a lipid dehydratase (39), led to sensitivity to LL37, indicating differences between the mechanisms of action of these two CAMPs, as previously suggested (16, 40). Taken together, these results support the notion that both CAMPs and ceragenins work by similar yet distinct mechanisms. These studies also provide a starting point for the genetic determination of the mode of action of ceragenins.

## DISCUSSION

Although ceragenins were designed to mimic the physicochemical properties of CAMPs (11, 12), our results indicated that they evoke different responses from bacteria than naturally occurring CAMPs. Our finding that ceragenins are active against a broader array of microbes than CAMPs, including mycobacteria, was our first indication that they have different mechanisms of action. Using transcriptomics, proteomics, and a CRISPRi genetic approach, we compared the responses of bacteria to CAMPs and ceragenins and revealed similarities, but also striking differences, and showed that ceragenins trigger a distinctive envelope stress response. Furthermore, our data also suggested that the two prototypical ceragenins, CSA13 and CSA131, trigger different responses in bacteria. Overall, while our results confirmed that ceragenins act on the bacterial envelope, they challenged the assumption that CAMPs and ceragenins share the same mechanism of action.

Profiling the responses of *E. coli* to CAMPs and ceragenins showed that these compounds trigger the Cpx envelope stress response, which is known to contribute to the bacterial adaptation to defects in the secretion and folding of the inner membrane and periplasmic proteins (21, 41). This corroborates previous studies demonstrating that the CpxR/CpxA system influences the susceptibility of bacteria to CAMPs (42, 43) and suggests that the Cpx response might similarly help bacteria survive exposure to ceragenins. The hypothesis that the envelope stress response is induced by CAMPs and ceragenins is also supported by the modulation of genes

associated with cis-acting elements for  $\sigma^E$  (Fig. 4A) and by the enrichment and/or depletion of CRISPRi strains targeting components of the bacterial envelope (Fig. 7). However, additional mechanistic studies are required to establish if regulators of the envelope stress response (e.g., CpxR, CpxA, and  $\sigma^E$ ) influence the susceptibility of *E. coli* to ceragenins and directly contribute to the bacterial response.

A striking similarity between the transcriptomic profiles of bacteria exposed to CAMPs and ceragenins is the downregulation of genes involved in the biosynthesis of purines and pyrimidines (Fig. 2K, 3C and D, 4B, and 5B). The cause of this downregulation is unknown, but it is possible that the repression of these metabolic pathways is part of the adaptive response to antibiotic exposure (44) and/or relates to a decreased requirement for nucleic acid in growth-inhibited bacteria. An intriguing question is whether the flux of the metabolites through these nucleotide metabolic pathways affects susceptibility to antimicrobial agents targeting the bacterial envelope, as observed for other antibiotics (45).

The results of this study showed that *E. coli* responds differently to CAMPs and ceragenins. We showed that CAMPs specifically induced the Rcs response and the expression of genes involved in the biosynthesis of colanic acid (Fig. 2J, 3A and B, 5C, and 6C and E). This is consistent with a previous study that demonstrated that CAMPs, including polymyxin B and LL37, induce the Rcs regulon through the outer membrane lipoprotein RcsF (46). Surprisingly, the ceragenins CSA13 and CSA131 did not induce the Rcs response as markedly as CAMPs (Fig. 5C). Thus, in contrast with the current model that outer membrane perturbation by CAMPs is required for the activation of the Rcs response by RcsF (46, 47), our results show that ceragenins perturb the bacterial envelope of *E. coli* without extensively triggering the Rcs response. We also found that ceragenins, but not CAMPs, induced the expression of genes involved in phosphate transport and of the PhoB regulon (Fig. 2J, 3A and B, 5D, and 6D). Although the reasons why these genes are differently modulated following exposure to antimicrobial compounds are not understood and warrant additional mechanistic studies, these results strongly suggest that ceragenins and CAMPs have distinctive mechanisms of action.

Despite some similarities between the response of bacteria exposed to ceragenins, such as the upregulation of several genes of the Cpx and PhoB regulons and the downregulation of genes involved in nucleotide metabolism, our data also showed striking differences between bacteria exposed to CSA13 and CSA131 (Fig. 2I to K and 7E). These differences include the upregulation of genes encompassing several functions (e.g., transcription factors and proteins involved in the heat response) as well as the downregulation of genes involved in protein translation in bacteria exposed to CSA13 (Fig. 2J and K). While the basis for these differences is unknown, as noted above, the LogP values of CSA13 and CSA131 are almost 2 orders of magnitude apart, suggesting that the level of hydrophobicity of the compounds may underlie their different effects. Given that the site of action is the bacterial envelope, such a significant difference in partition coefficient values is likely to alter responses to membrane targets, especially the extremely hydrophobic outer membrane of mycobacteria. Interestingly, results from a previous study demonstrated that, unlike other ceragenins, CSA13 can permeabilize both the outer and inner membranes of *E. coli* (14). Although CSA131 was not included in this previous study, one hypothesis is that differences in membrane permeabilization by CSA13 and CSA131 have an impact on the bacterial response to these antimicrobials. Future work exploring the response of bacteria to a broader range of ceragenins will help in understanding these differences and might guide the design of compounds with a more specific mode of action.

Our CRISPRi approach identified sensitizing interactions between genes involved in the biology of the bacterial envelope and the antibacterial compounds colistin, LL37, CSA13, and CSA131 (Fig. 7). This information might prove valuable for the design of combination therapies that are synergistic and prevent the emergence of resistance but also allow treatment regimens with lower concentrations of antibiotics and dose-related antibiotic toxicity (48–50). As an example, triclosan, a compound that inhibits

the ceragenin-sensitivity determinant FabI (51) (Fig. 7E), might synergize with ceragenins by altering the properties of the bacterial envelope and sensitizing bacteria to the action of ceragenins. As another example, the CAMPs/ceragenins-sensitivity determinant LpxB was suggested as a target for the development of antibacterial compounds (52), which compounds would have the potential to synergize with CAMPs and ceragenins more broadly (Fig. 7E), assuming that the target for CAMPs and ceragenins is not LpxB. Although those antibacterial interactions are purely speculative, our results suggest that CRISPRi approaches could be valuable tools for target identification and the development of antibiotic combination therapies.

The results of this study suggested that CAMPs and ceragenins both kill bacteria by targeting the bacterial envelope. However, this study also supports the hypothesis that ceragenins have a distinctive mode of action and we propose a model in which ceragenins cross the outer layers of the bacterial envelope and target more specifically the inner membrane. This hypothesis is supported by the broad spectrum of action of these molecules, which extend beyond bacteria. Whether the broader activity range of ceragenins impacts the selectivity for microbial membranes characteristic of endogenous CAMPs remains a key question for future study. A better understanding of the structure-activity relationship of these compounds and a deeper knowledge of their unique mechanism of action will be essential in the discovery of the next generation of ceragenins with increased potency and selectivity. Future studies should also focus on characterizing the response and the genetic determinants of resistance to ceragenins in mycobacteria and Gram-positive bacteria as the identification of the target(s) of ceragenins may lead to the development of broad-spectrum therapeutics against bacterial diseases.

## MATERIALS AND METHODS

**Antimicrobial compounds.** CSA13 and CSA131 (53) as well as CSA44 and CSA144 (54) were prepared as described previously and solubilized at 10 mg/mL in sterile distilled and deionized (DD) water. LL37 (Anaspec, Fremont, CA, USA), colistin (Sigma-Aldrich, St-Louis, MO, USA), and ciprofloxacin (MP Biomedicals, Irvine, CA, USA) were solubilized at 10 mg/mL in sterile DD water. Erythromycin (Sigma-Aldrich) was solubilized at 10 mg/mL in ethanol. Antimicrobial compounds were aliquoted and stored at  $-20^{\circ}\text{C}$ . Freeze-thaw cycles of stock solutions were limited to three times.

**Bacterial strains and growth conditions.** *E. coli* MG1655 (55), *L. monocytogenes* 10403S (56), *M. marinum* strain M (57), *M. smegmatis* mc<sup>2</sup>155 (58), and *M. tuberculosis* Erdman (57) were as previously described. *M. avium* mc<sup>2</sup>2500 is a clinical strain isolated from an AIDS patient with pulmonary disease and predominantly formed a smooth/transparent colony morphotype on solid agar (15). *M. avium* mc<sup>2</sup>2500D is an isogenic, laboratory-derived strain with an opaque colony morphotype. *E. coli* and *L. monocytogenes* were routinely grown on Mueller-Hinton agar (MHA) (BD, Franklin Lakes, NJ, USA) plates or in cation-adjusted Mueller-Hinton (CAMH) (BD) broth and on Brain-heart infusion agar (BHIA) (Becton, Dickinson) plates or in Brain-heart infusion (BHI) (BD) broth, respectively. *M. avium* and *M. tuberculosis* were cultured in Middlebrook 7H9 (BD) broth containing 0.5% glycerol, 10% Oleic Albumin Dextrose Catalase (OADC) (Sigma-Aldrich), and 0.05% Tween 80. *M. marinum* was cultured in Middlebrook 7H9 broth containing 0.5% glycerol, 10% OADC, and 0.2% Tween 80. *M. smegmatis* was grown on Middlebrook 7H10 (BD) plates or Middlebrook 7H9 broth containing 0.5% glycerol, 0.5% dextrose, and 0.2% Tween 80 unless otherwise stated. All bacterial strains were grown at  $37^{\circ}\text{C}$ , except *M. marinum*, which was grown at  $30^{\circ}\text{C}$ . Liquid cultures were incubated with shaking unless otherwise stated.

**Antibiotic susceptibility testing.** MICs of antimicrobial compounds against *E. coli* and *L. monocytogenes* were determined by a broth microdilution technique following the recommendations of the Clinical and Laboratory Standards Institute (CLSI) (59), except that BHI was used to perform assays on *L. monocytogenes*. Antibiotic quality control experiments were performed using *E. coli* ATCC25922 (ATCC, Manassas, VA, USA). A similar protocol using extended incubation periods was used to determine MICs against *M. avium* (10 days), *M. marinum* (5 days), *M. smegmatis* (3 days), and *M. tuberculosis* (14 days). For the determination of MICs using mycobacterial species, plates were placed in a vented container containing damp wipes to minimize evaporation.

**Time-kill experiments.** Time-kill experiments were performed to characterize the effect of compounds on bacterial growth and survival. Bacteria were inoculated at  $10^5$  to  $10^6$  colony forming units (CFU)/mL in liquid media in the absence or presence of antibiotics at the following concentrations: *E. coli*, 0.5  $\mu\text{g}/\text{mL}$  colistin, 64  $\mu\text{g}/\text{mL}$  LL37, 4  $\mu\text{g}/\text{mL}$  CSA13 and 4  $\mu\text{g}/\text{mL}$  CSA131; *L. monocytogenes*, 2  $\mu\text{g}/\text{mL}$  CSA13, 2  $\mu\text{g}/\text{mL}$  CSA131, 2  $\mu\text{g}/\text{mL}$  ciprofloxacin and 0.25  $\mu\text{g}/\text{mL}$  erythromycin; *M. smegmatis*, 0.5  $\mu\text{g}/\text{mL}$  CSA13 and 0.5  $\mu\text{g}/\text{mL}$  ciprofloxacin. Bacterial cultures were grown at  $37^{\circ}\text{C}$  with shaking and the number of CFU/mL was determined at several time points. Plates without Tween 80 were used for the CFU determination of *M. smegmatis* cultures.

**Serial passage experiments.** Serial passage of bacteria in the presence of subinhibitory concentrations was performed as previously described (13, 60). Experiments were performed in CAMH or BHI broth for *E.*

*coli* and *L. monocytogenes*, respectively. In a few cases, bacteria growing at the two highest subinhibitory concentrations of antimicrobial had to be combined to get inoculums of  $10^5$  to  $10^6$  CFU/mL.

**Preparation and sampling of bacterial cultures for transcriptomic profiling.** A single colony of *E. coli* MG1655 was inoculated into CAMH broth and incubated for 16 to 18 h at 37°C with shaking. Cultures were diluted in fresh media to an absorbance at 600 nm ( $A_{600}$ ) of 0.1, incubated at 37°C with shaking until an  $A_{600}$  of 0.8 to 1.0 (~2 h) and antibiotics were added to each culture, which was further incubated for 1 h at 37°C with shaking. Antibiotics were adjusted to concentrations having a similar impact on *E. coli* growth for that particular, higher bacterial density, culture format (i.e., 4  $\mu$ g/mL colistin, 8  $\mu$ g/mL CSA13, 8  $\mu$ g/mL CSA131, and 256  $\mu$ g/mL LL37). Cultures samples were then mixed 1:2 with RNA Protect Bacteria Reagent (Qiagen, Germantown, MD, USA), vortexed immediately for 5 s, and incubated for 5 min at room temperature. The bacterial suspensions were centrifuged for 10 min at  $5,000 \times g$ , supernatants were discarded, and pellets were stored a few days at  $-80^\circ\text{C}$  before proceeding to RNA extraction.

**RNA purification and sequencing.** Bacterial pellets were resuspended in 100  $\mu$ L of 10 mM Tris, 1 mM EDTA, pH 8.0 buffer containing 10 mg/mL lysozyme (Sigma-Aldrich). Proteinase K (New England Biolabs, Ipswich, MA, USA) (2.5  $\mu$ L of 20 mg/mL) was added and samples were incubated at room temperature for 10 min with frequent mixing. Samples were combined with 0.5  $\mu$ L of 10% SDS and 350  $\mu$ L of lysis buffer (Ambion life technologies, Invitrogen, Carlsbad, CA, USA) containing  $\beta$ -mercaptoethanol, vortexed and lysates were transferred into 1.5 mL RNase-free microcentrifuge tubes. Samples were then passed 5 times through an 18 to 21-gauge needle and centrifuged at  $12,000 \times g$  for 2 min at room temperature. Supernatants were transferred to new 1.5 mL RNase-free microcentrifuge tubes before proceeding to the washing and elution steps described in the PureLink RNA minikit (Ambion Life Technologies). Samples were treated with DNase (New England Biolabs) for 15 min at 37°C in a volume of 50  $\mu$ L and 5  $\mu$ L of 25 mM EDTA was added. Samples were further incubated for 10 min at 75°C and quickly placed on ice before being cleaned and reloaded using the RNA Clean & Concentrator kit (Zymo Research, Irvine, CA, USA) and stored at  $-80^\circ\text{C}$ . The quality and the quantity of each RNA sample were analyzed by the UC Berkeley QB3 facility using a bioanalyzer and the Qubit technology. RNA samples were sequenced and preliminarily analyzed by the University of California (UC) Davis Genome Center and the UC Davis Bioinformatics Core.

**Analysis of RNAseq data.** The differential expression analyses were conducted using the limma-voom Bioconductor pipeline (61) (EdgeR version 3.20.9, limma version 3.34.9) and R 3.4.4 by the UC Davis Bioinformatics Core. The multidimensional plot was created using the EdgeR function plotMDS. Pathway analyses were performed using DAVID Bioinformatics Resources 6.8 (62, 63). Only annotation terms from the following databases were included: UP (UniProt) Keywords, COG (cluster of orthologous groups) Ontology, GO (gene ontology for biological process, molecular function, and cellular component), and KEGG. Venn diagram analyses were performed using the tool provided on the Bioinformatics & Evolutionary Genomics website of Ghent University (64). Promoter and regulatory binding analyses were performed using the Gene Expression Analysis Tools (20). Only one repeated binding site and promoter was considered for each gene for any specific transcription factors to avoid redundancy. Lists of genes to be included in specific regulons were retrieved from the RegulonDB Database (65). Fold changes for few transcripts of regulons CpxR (*cpxQ*, *csgC*, *cyaR*, *efeU*, *rprA*, *rseD*), PurR (*codA*, *codB*) and PhoB (*cusC*, *phnE*, *prpR*) were not included in this analysis. The information related to the expected activity (induction and/or repression) of each transcription factor on specific genes was also retrieved from the RegulonDB Database.

**Protein extraction and peptide preparation from *E. coli* cultures.** A single colony of *E. coli* MG1655 was inoculated into CAMH broth and incubated for 16 to 18 h at 37°C with shaking. Cultures were diluted in fresh media to an  $A_{600}$  of 0.1, incubated at 37°C with shaking until an  $A_{600}$  of 0.8 to 1.0 (~2 h) and antibiotics (4  $\mu$ g/mL colistin or 8  $\mu$ g/mL CSA13) were then added to each culture, which was further incubated for 3 h at 37°C with shaking. Protein was extracted, digested, and desalted, as previously described (66), with few modifications. Briefly, 23 mL of the bacterial cultures were washed twice in cold PBS and resuspended in 4 mL of lysis buffer (8 M urea, 150 mM NaCl, 100 mM ammonium bicarbonate, pH 8) containing Roche mini-complete protease inhibitor EDTA-free and Roche PhosSTOP (1 tablet of each per 10 mL of buffer) (Roche, Basel, Switzerland). Samples (on ice) were then sonicated 10 times with a Sonics VibraCell probe tip sonicator at 7 W for 10 s. Insoluble precipitates were removed from lysates using a 30 min centrifugation at  $\sim 16,100 \times g$  at 4°C and the protein concentration of each lysate was determined using the microplate procedure of the Micro BCA™ Protein assay kit (Thermo Fischer Scientific, Emeryville, CA, USA). Clarified lysates (1 mg each) were reduced with 4 mM tris(2-carboxyethyl)phosphine for 30 min at room temperature, alkylated with 10 mM iodoacetamide for 30 min at room temperature in the dark, and quenched with 10 mM 1,4-dithiothreitol for 30 min at room temperature in the dark. Samples were diluted with three volumes of 100 mM ammonium bicarbonate, pH 8.0, and incubated with 10  $\mu$ g of sequencing grade modified trypsin (Promega, Madison, WI, USA) while rotating at room temperature for 18 h. Trifluoroacetic acid (TFA) was then added to a final concentration of 0.3% to each sample, followed by 1:100 of 6 M HCl and the removal of insoluble material by centrifugation at  $\sim 2,000 \times g$  for 10 min. SepPak C18 solid-phase extraction cartridges (Waters, Milford, MA, USA) were activated with 1 mL of 80% acetonitrile (ACN), 0.1% TFA, and equilibrated with 3 mL of 0.1% TFA. Peptides were desalted by applying samples to equilibrated columns, followed by a washing step with 3 mL of 0.1% TFA and elution with 1.1 mL of 40% ACN, 0.1% TFA. The subsequent global protein analysis was performed using 10  $\mu$ g of each desalted peptide sample.

**Liquid chromatography, mass spectrometry, label-free quantification, and analysis of the proteomic data.** Peptides were analyzed using liquid chromatography and mass spectrometry, as previously described (66). Mass spectrometry data were assigned to *E. coli* sequences and MS1 intensities were extracted with MaxQuant (version 1.6.0.16) (67). Data were searched against the *E. coli* (strain K-12) protein database (downloaded on November 6, 2018). MaxQuant settings were left at the default except

for that trypsin (KR|P) was selected, allowing for up to two missed cleavages. Data were then further analyzed with the artMS Bioconductor package (68), using the MSstats Bioconductor package (version 3.14.1) (69) and the artMS version 0.9. Contaminants and decoy hits were removed, and samples were normalized across fractions by median-centering the  $\log_2$ -transformed MS1 intensity distributions. The MSstats group comparison function was run with no interaction terms for missing values, no interference, unequal intensity feature variance as well as the restricted technical and biological scope of replication.  $\log_2$ -fold change for proteins/sites with missing values in one condition but found in >2 biological replicates of the other condition of any given comparison were estimated by imputing intensity values from the lowest observed MS1-intensity across samples (68), and *P* values were randomly assigned between 0.05 and 0.01 for illustration purposes. Pathway and Venn diagram analyses were performed as described for the analysis of RNAseq data.

**Identification of genetic determinants of resistance to antibiotics using clustered regularly interspaced short palindromic repeats interference (CRISPRi).** A pooled CRISPRi library of ~500 strains that allow the inducible knockdown of genes predicted to be essential was used to study the genetic determinants of resistance to CAMPs and ceragenins, as previously described (30), with few modifications. To quantify the antibiotic sensitivity of each CRISPRi strain, the relative proportion of each sgRNA spacer in the mixed population was enumerated by deep sequencing, after 15 doublings in the presence of saturating IPTG and 0.031  $\mu\text{g}/\text{mL}$  colistin, 12  $\mu\text{g}/\text{mL}$  LL37, 0.5  $\mu\text{g}/\text{mL}$  CSA13 or 0.25  $\mu\text{g}/\text{mL}$  CSA131. Experiments were run in parallel for two studies, and a detailed description of Materials and Methods as well as data for the untreated controls with or without IPTG-induction was described previously (30).

**Determination of log(P) values.** Log *P* values (partition coefficient) were determined using Chemicalize from ChemAxon (Escondido, CA, USA).

**Preparation of graphs.** GraphPad Prism software (v.7.00) was used to generate graphs and perform statistical tests. The number of independent experiments is indicated in each figure legend.

**Data availability.** RNAseq data were deposited in the GEO repository under the GEO accession number [GSE160082](https://www.ncbi.nlm.nih.gov/geo/query/acc.cgi?acc=GSE160082). DNA sequencing data obtained with the pooled CRISPRi library were deposited in the Short Read Archive under accession number [PRJNA669343](https://www.ncbi.nlm.nih.gov/sra/PRJNA669343). The mass spectroscopy proteomics data were deposited to the ProteomeXchange Consortium via the PRIDE (70) partner repository with the dataset identifier [PXD022149](https://www.ebi.ac.uk/pride/archive/study/PXD022149).

## SUPPLEMENTAL MATERIAL

Supplemental material is available online only.

**DATA SET S1**, XLSX file, 1.7 MB.

**DATA SET S2**, XLSX file, 0.5 MB.

**DATA SET S3**, XLSX file, 0.1 MB.

**DATA SET S4**, XLSX file, 0.04 MB.

**DATA SET S5**, XLSX file, 0.2 MB.

**DATA SET S6**, XLSX file, 0.1 MB.

**DATA SET S7**, XLSX file, 0.1 MB.

**TABLE S1**, PDF file, 0.01 MB.

**TABLE S2**, PDF file, 0.3 MB.

**TABLE S3**, PDF file, 0.1 MB.

## ACKNOWLEDGMENTS

We thank Teresa Repasy and Guillaume Golovkine for their assistance during the design of the RNAseq experiments, and Daniel A. Portnoy for providing *L. monocytogenes* 10403S. We acknowledge help from the UC Berkeley Functional Genomics Laboratory, the UC Davis Genome Center, and the UC Davis Bioinformatics Core in performing and analyzing RNAseq experiments as well as the Chan Zuckerberg Biohub for the sequencing of the CRISPRi libraries. The UC Berkeley proteomics core assisted with the liquid chromatography-mass spectrometry (LC-MS) analysis of our peptide samples.

J.M.B. was supported by NIH training grants (4T32HL007185-39, 4T32HL007185-40, 5K12HL119997-05, and 1K08AI146267-0) and a Cystic Fibrosis Foundation Harry Shwachman Award. This work was supported in part by the Ceragenin Research Fund granted to M.A.M. and J.S.C. by Bill Brown and Sharon Bonner-Brown.

We declare no conflict of interest.

## REFERENCES

1. World Health Organization. 2014. Antimicrobial resistance: global report on surveillance 2014. World Health Organization, Geneva, Switzerland.
2. World Health Organization. 2019. Global tuberculosis report 2019. World Health Organization, Geneva, Switzerland.



3. Coates AR, Halls G, Hu Y. 2011. Novel classes of antibiotics or more of the same? *Br J Pharmacol* 163:184–194. <https://doi.org/10.1111/j.1476-5381.2011.01250.x>.
4. Silver LL. 2011. Challenges of antibacterial discovery. *Clin Microbiol Rev* 24:71–109. <https://doi.org/10.1128/CMR.00030-10>.
5. Tommasi R, Brown DG, Walkup GK, Manchester JJ, Miller AA. 2015. ESKA-PEing the labyrinth of antibacterial discovery. *Nat Rev Drug Discov* 14:529–542. <https://doi.org/10.1038/nrd4572>.
6. Bradshaw J. 2003. Cationic antimicrobial peptides: issues for potential clinical use. *BioDrugs* 17:233–240. <https://doi.org/10.2165/00063030-200317040-00002>.
7. Brogden KA. 2005. Antimicrobial peptides: pore formers or metabolic inhibitors in bacteria? *Nat Rev Microbiol* 3:238–250. <https://doi.org/10.1038/nrmicro1098>.
8. Sochacki KA, Barns KJ, Bucki R, Weisshaar JC. 2011. Real-time attack on single *Escherichia coli* cells by the human antimicrobial peptide LL-37. *Proc Natl Acad Sci U S A* 108:E77–E81. <https://doi.org/10.1073/pnas.1101130108>.
9. Omardien S, Brul S, Zaat SA. 2016. Antimicrobial Activity of Cationic Antimicrobial Peptides against Gram-Positives: current Progress Made in Understanding the Mode of Action and the Response of Bacteria. *Front Cell Dev Biol* 4:111. <https://doi.org/10.3389/fcell.2016.00111>.
10. Pfalzgraff A, Brandenburg K, Weindl G. 2018. Antimicrobial Peptides and Their Therapeutic Potential for Bacterial Skin Infections and Wounds. *Front Pharmacol* 9:281. <https://doi.org/10.3389/fphar.2018.00281>.
11. Hashemi MM, Holden BS, DurnaAA B, Buck R, Savage PB. 2017. Ceragenins as mimics of endogenous antimicrobial peptides. *J Antimicrob Agents* 3:2472–1212. <https://doi.org/10.4172/2472-1212.1000141>.
12. Li C, Peters AS, Meredith EL, Allman GW, Savage PB. 1998. Design and Synthesis of Potent Sensitizers of Gram-Negative Bacteria Based on a Cholic Acid Scaffolding. *J Am Chem Soc* 120:2961–2962. <https://doi.org/10.1021/ja973881r>.
13. Pollard JE, Snarr J, Chaudhary V, Jennings JD, Shaw H, Christiansen B, Wright J, Jia W, Bishop RE, Savage PB. 2012. In vitro evaluation of the potential for resistance development to ceragenin CSA-13. *J Antimicrob Chemother* 67:2665–2672. <https://doi.org/10.1093/jac/dks276>.
14. Epanand RF, Pollard JE, Wright JO, Savage PB, Epanand RM. 2010. Depolarization, bacterial membrane composition, and the antimicrobial action of ceragenins. *Antimicrob Agents Chemother* 54:3708–3713. <https://doi.org/10.1128/AAC.00380-10>.
15. Otero J, Jacobs WR, Jr, Glickman MS. 2003. Efficient allelic exchange and transposon mutagenesis in *Mycobacterium avium* by specialized transduction. *Appl Environ Microbiol* 69:5039–5044. <https://doi.org/10.1128/AEM.69.9.5039-5044.2003>.
16. Pristovsek P, Kidric J. 1999. Solution structure of polymyxins B and E and effect of binding to lipopolysaccharide: an NMR and molecular modeling study. *J Med Chem* 42:4604–4613. <https://doi.org/10.1021/jm991031b>.
17. Dominguez A, Munoz E, Lopez MC, Cordero M, Martinez JP, Vinas M. 2017. Transcriptomics as a tool to discover new antibacterial targets. *Bio-technol Lett* 39:819–828. <https://doi.org/10.1007/s10529-017-2319-0>.
18. Briffotiaux J, Liu S, Gicquel B. 2019. Genome-Wide Transcriptional Responses of *Mycobacterium* to Antibiotics. *Front Microbiol* 10:249. <https://doi.org/10.3389/fmicb.2019.00249>.
19. Price NL, Raivio TL. 2009. Characterization of the Cpx regulon in *Escherichia coli* strain MC4100. *J Bacteriol* 191:1798–1815. <https://doi.org/10.1128/JB.00798-08>.
20. Huerta AM, Glasner JD, Gutiérrez-Ríos RM, Blattner FR, Collado-Vides J. 2002. GETools: gene expression tool for analysis of transcriptome experiments in *E. coli*. *Trends in Genetics* 18:217–218. [https://doi.org/10.1016/S0168-9525\(01\)02620-8](https://doi.org/10.1016/S0168-9525(01)02620-8).
21. Mitchell AM, Silhavy TJ. 2019. Envelope stress responses: balancing damage repair and toxicity. *Nat Rev Microbiol* 17:417–428. <https://doi.org/10.1038/s41579-019-0199-0>.
22. Jishage M, Iwata A, Ueda S, Ishihama A. 1996. Regulation of RNA polymerase sigma subunit synthesis in *Escherichia coli*: intracellular levels of four species of sigma subunit under various growth conditions. *J Bacteriol* 178:5447–5451. <https://doi.org/10.1128/jb.178.18.5447-5451.1996>.
23. Sun Z, Cagliero C, Izard J, Chen Y, Zhou YN, Heinz WF, Schneider TD, Jin DJ. 2019. Density of sigma70 promoter-like sites in the intergenic regions dictates the redistribution of RNA polymerase during osmotic stress in *Escherichia coli*. *Nucleic Acids Res* 47:3970–3985. <https://doi.org/10.1093/nar/gkz159>.
24. Erickson JW, Gross CA. 1989. Identification of the sigma E subunit of *Escherichia coli* RNA polymerase: a second alternate sigma factor involved in high-temperature gene expression. *Genes Dev* 3:1462–1471. <https://doi.org/10.1101/gad.3.9.1462>.
25. Alba BM, Gross CA. 2004. Regulation of the *Escherichia coli* sigma-dependent envelope stress response. *Mol Microbiol* 52:613–619. <https://doi.org/10.1111/j.1365-2958.2003.03982.x>.
26. Nonaka G, Blankschien M, Herman C, Gross CA, Rhodius VA. 2006. Regulon and promoter analysis of the *E. coli* heat-shock factor, sigma32, reveals a multifaceted cellular response to heat stress. *Genes Dev* 20:1776–1789. <https://doi.org/10.1101/gad.1428206>.
27. Rolfes RJ, Zalkin H. 1988. *Escherichia coli* gene purR encoding a repressor protein for purine nucleotide synthesis. Cloning, nucleotide sequence, and interaction with the purF operator. *J Biol Chem* 263:19653–19661. [https://doi.org/10.1016/S0021-9258\(19\)77686-8](https://doi.org/10.1016/S0021-9258(19)77686-8).
28. Cho BK, Federowicz SA, Emtree M, Park YS, Kim D, Palsson BO. 2011. The PurR regulon in *Escherichia coli* K-12 MG1655. *Nucleic Acids Res* 39:6456–6464. <https://doi.org/10.1093/nar/gkr307>.
29. Lamarche MG, Wanner BL, Crepin S, Harel J. 2008. The phosphate regulon and bacterial virulence: a regulatory network connecting phosphate homeostasis and pathogenesis. *FEMS Microbiol Rev* 32:461–473. <https://doi.org/10.1111/j.1574-6976.2008.00101.x>.
30. Silvis MR, Rajendram M, Shi H, Osadnik H, Gray AN, Cesar S, Peters JM, Hearne CC, Kumar P, Todor H, Huang KC, Gross CA. 2021. Morphological and Transcriptional Responses to CRISPRi Knockdown of Essential Genes in *Escherichia coli*. *mBio* 12:e0256121. <https://doi.org/10.1128/mBio.02561-21>.
31. Peters JM, Colavin A, Shi H, Czarny TL, Larson MH, Wong S, Hawkins JS, Lu CHS, Koo BM, Marta E, Shiver AL, Whitehead EH, Weissman JS, Brown ED, Qi LS, Huang KC, Gross CA. 2016. A Comprehensive, CRISPR-based Functional Analysis of Essential Genes in Bacteria. *Cell* 165:1493–1506. <https://doi.org/10.1016/j.cell.2016.05.003>.
32. Metzger LEt, Raetz CR. 2009. Purification and characterization of the lipid A disaccharide synthase (LpxB) from *Escherichia coli*, a peripheral membrane protein. *Biochemistry* 48:11559–11571. <https://doi.org/10.1021/bi901750f>.
33. Narita S, Tokuda H. 2009. Biochemical characterization of an ABC transporter LptBFGC complex required for the outer membrane sorting of lipopolysaccharides. *FEBS Lett* 583:2160–2164. <https://doi.org/10.1016/j.febslet.2009.05.051>.
34. Biswas T, Yi L, Aggarwal P, Wu J, Rubin JR, Stuckey JA, Woodard RW, Tsodikov OV. 2009. The tail of KdsC: conformational changes control the activity of a haloacid dehalogenase superfamily phosphatase. *J Biol Chem* 284:30594–30603. <https://doi.org/10.1074/jbc.M109.012278>.
35. Hajj Chehade M, Pelosi L, Fyfe CD, Loiseau L, Rascalou B, Brugiere S, Kazemzadeh K, Vo CD, Ciccone L, Aussel L, Couste Y, Fontecave M, Barras F, Lombard M, Pierrel F. 2019. A Soluble Metabolite Synthesizes the Isoprenoid Lipid Ubiquinone. *Cell Chem Biol* 26:482–492.e7. <https://doi.org/10.1016/j.chembiol.2018.12.001>.
36. Bergler H, Fuchsbichler S, Hogenauer G, Turnowsky F. 1996. The enoyl-[acyl-carrier-protein] reductase (FabI) of *Escherichia coli*, which catalyzes a key regulatory step in fatty acid biosynthesis, accepts NADH and NADPH as cofactors and is inhibited by palmitoyl-CoA. *Eur J Biochem* 242:689–694. <https://doi.org/10.1111/j.1432-1033.1996.0689r.x>.
37. Heath RJ, Rock CO. 1995. Enoyl-acyl carrier protein reductase (fabI) plays a determinant role in completing cycles of fatty acid elongation in *Escherichia coli*. *J Biol Chem* 270:26538–26542. <https://doi.org/10.1074/jbc.270.44.26538>.
38. Rawlings M, Cronan JE, Jr. 1992. The gene encoding *Escherichia coli* acyl carrier protein lies within a cluster of fatty acid biosynthetic genes. *J Biol Chem* 267:5751–5754. [https://doi.org/10.1016/S0021-9258\(18\)42616-6](https://doi.org/10.1016/S0021-9258(18)42616-6).
39. Heath RJ, Rock CO. 1996. Roles of the FabA and FabZ beta-hydroxyacyl-acyl carrier protein dehydratases in *Escherichia coli* fatty acid biosynthesis. *J Biol Chem* 271:27795–27801. <https://doi.org/10.1074/jbc.271.44.27795>.
40. Turner J, Cho Y, Dinh NN, Waring AJ, Lehrer R. 1998. Activities of LL-37, a cathelin-associated antimicrobial peptide of human neutrophils. *Antimicrob Agents Chemother* 42:2206–2214. <https://doi.org/10.1128/AAC.42.9.2206>.
41. Raivio TL. 2014. Everything old is new again: an update on current research on the Cpx envelope stress response. *Biochim Biophys Acta* 1843:1529–1541. <https://doi.org/10.1016/j.bbamcr.2013.10.018>.
42. Audrain B, Ferrieres L, Zairi A, Soubigou G, Dobson C, Coppee JY, Beloin C, Ghigo JM. 2013. Induction of the Cpx envelope stress pathway contributes to *Escherichia coli* tolerance to antimicrobial peptides. *Appl Environ Microbiol* 79:7770–7779. <https://doi.org/10.1128/AEM.02593-13>.
43. Weatherspoon-Griffin N, Zhao G, Kong W, Kong Y, Morigen Andrews-Polymenis H, McClelland M, Shi Y. 2011. The CpxR/CpxA two-component system up-regulates two Tat-dependent peptidoglycan amidases to confer bacterial resistance to antimicrobial peptide. *J Biol Chem* 286:5529–5539. <https://doi.org/10.1074/jbc.M110.200352>.

44. Zampieri M, Zimmermann M, Claassen M, Sauer U. 2017. Nontargeted Metabolomics Reveals the Multilevel Response to Antibiotic Perturbations. *Cell Rep* 19:1214–1228. <https://doi.org/10.1016/j.celrep.2017.04.002>.
45. Yang JH, Wright SN, Hamblin M, McCloskey D, Alcantar MA, Schrubbers L, Lopatkin AJ, Satish S, Nili A, Palsson BO, Walker GC, Collins JJ. 2019. A White-Box Machine Learning Approach for Revealing Antibiotic Mechanisms of Action. *Cell* 177:1649–1661.e9. <https://doi.org/10.1016/j.cell.2019.04.016>.
46. Farris C, Sanowar S, Bader MW, Pfuetschner R, Miller SI. 2010. Antimicrobial peptides activate the Rcs regulon through the outer membrane lipoprotein RcsF. *J Bacteriol* 192:4894–4903. <https://doi.org/10.1128/JB.00505-10>.
47. Konovalova A, Mitchell AM, Silhavy TJ. 2016. A lipoprotein/beta-barrel complex monitors lipopolysaccharide integrity transducing information across the outer membrane. *Elife* 5:e15276. <https://doi.org/10.7554/eLife.15276>.
48. Zheng W, Sun W, Simeonov A. 2018. Drug repurposing screens and synergistic drug-combinations for infectious diseases. *Br J Pharmacol* 175:181–191. <https://doi.org/10.1111/bph.13895>.
49. Zimmermann GR, Lehar J, Keith CT. 2007. Multi-target therapeutics: when the whole is greater than the sum of the parts. *Drug Discov Today* 12: 34–42. <https://doi.org/10.1016/j.drudis.2006.11.008>.
50. Moellering RC, Jr. 1983. Rationale for use of antimicrobial combinations. *Am J Med* 75:4–8. [https://doi.org/10.1016/0002-9343\(83\)90088-8](https://doi.org/10.1016/0002-9343(83)90088-8).
51. Heath RJ, Rubin JR, Holland DR, Zhang E, Snow ME, Rock CO. 1999. Mechanism of triclosan inhibition of bacterial fatty acid synthesis. *J Biol Chem* 274:11110–11114. <https://doi.org/10.1074/jbc.274.16.11110>.
52. Bohl TE, Shi K, Lee JK, Aihara H. 2018. Crystal structure of lipid A disaccharide synthase LpxB from *Escherichia coli*. *Nat Commun* 9:377. <https://doi.org/10.1038/s41467-017-02712-9>.
53. Li C, Budge LP, Driscoll CD, Willardson BM, Allman GW, Savage PB. 1999. Incremental conversion of outer-membrane permeabilizers into potent antibiotics for Gram-negative bacteria. *J Am Chem Soc* 121:931–940. <https://doi.org/10.1021/ja982938m>.
54. Guan Q, Li C, Schmidt EJ, Boswell JS, Walsh JP, Allman GW, Savage PB. 2000. Preparation and characterization of cholic acid-derived antimicrobial agents with controlled stabilities. *Org Lett* 2:2837–2840. <https://doi.org/10.1021/ol0062704>.
55. Lim B, Miyazaki R, Neher S, Siegele DA, Ito K, Walter P, Akiyama Y, Yura T, Gross CA. 2013. Heat shock transcription factor sigma32 co-opts the signal recognition particle to regulate protein homeostasis in *E. coli*. *PLoS Biol* 11:e1001735. <https://doi.org/10.1371/journal.pbio.1001735>.
56. Becavin C, Bouchier C, Lechat P, Archambaud C, Creno S, Gouin E, Wu Z, Kuhbacher A, Brisse S, Pucciarelli MG, Garcia-del Portillo F, Hain T, Portnoy DA, Chakraborty T, Lecuit M, Pizarro-Cerda J, Moszer I, Bierne H, Cossart P. 2014. Comparison of widely used *Listeria monocytogenes* strains EGD, 10403S, and EGD-e highlights genomic variations underlying differences in pathogenicity. *mBio* 5:e00969-14–e00914. <https://doi.org/10.1128/mBio.00969-14>.
57. Champion PA, Champion MM, Manzanillo P, Cox JS. 2009. ESX-1 secreted virulence factors are recognized by multiple cytosolic AAA ATPases in pathogenic mycobacteria. *Mol Microbiol* 73:950–962. <https://doi.org/10.1111/j.1365-2958.2009.06821.x>.
58. Snapper SB, Melton RE, Mustafa S, Kieser T, Jacobs WR, Jr. 1990. Isolation and characterization of efficient plasmid transformation mutants of *Mycobacterium smegmatis*. *Mol Microbiol* 4:1911–1919. <https://doi.org/10.1111/j.1365-2958.1990.tb02040.x>.
59. Clinical and Laboratory Standards Institute. 2018. Methods for dilution antimicrobial susceptibility tests for bacteria that grow aerobically. Approved standard. 11th edition. Clinical and Laboratory Standards Institute, Wayne, PA.
60. Lamontagne Boulet M, Isabelle C, Guay I, Brouillette E, Langlois JP, Jacques PE, Rodrigue S, Brzezinski R, Beauregard PB, Bouarab K, Boyapelly K, Boudreault PL, Marsault E, Malouin F. 2018. Tomatidine Is a Lead Antibiotic Molecule That Targets *Staphylococcus aureus* ATP Synthase Subunit C. *Antimicrob Agents Chemother* 62:e02197-17. <https://doi.org/10.1128/AAC.02197-17>.
61. Ritchie ME, Phipson B, Wu D, Hu Y, Law CW, Shi W, Smyth GK. 2015. limma powers differential expression analyses for RNA-sequencing and microarray studies. *Nucleic Acids Res* 43:e47. <https://doi.org/10.1093/nar/gkv007>.
62. Huang da W, Sherman BT, Lempicki RA. 2009. Bioinformatics enrichment tools: paths toward the comprehensive functional analysis of large gene lists. *Nucleic Acids Res* 37:1–13. <https://doi.org/10.1093/nar/gkn923>.
63. Huang DW, Sherman BT, Lempicki RA. 2009. Systematic and integrative analysis of large gene lists using DAVID Bioinformatics Resources. *Nat Protoc* 4:44–57. <https://doi.org/10.1038/nprot.2008.211>.
64. Bioinformatics and Evolutionary Genomics. Calculate and draw custom Venn diagrams. <http://bioinformatics.psb.ugent.be/webtools/Venn/>. Accessed 2020-02-01.
65. Santos-Zavaleta A, Salgado H, Gama-Castro S, Sanchez-Perez M, Gomez-Romero L, Ledezma-Tejeda D, Garcia-Sotelo JS, Alquicira-Hernandez K, Muniz-Rascado LJ, Pena-Loredo P, Ishida-Gutierrez C, Velazquez-Ramirez DA, Del Moral-Chavez V, Bonavides-Martinez C, Mendez-Cruz CF, Galagan J, Collado-Vides J. 2019. RegulonDB v 10.5: tackling challenges to unify classic and high throughput knowledge of gene regulation in *E. coli* K-12. *Nucleic Acids Res* 47:D212–D220. <https://doi.org/10.1093/nar/gky1077>.
66. Budzik JM, Swaney DL, Jimenez-Morales D, Johnson JR, Garelis NE, Repasy T, Roberts AW, Popov LM, Parry TJ, Pratt D, Ideker T, Krogan NJ, Cox JS. 2020. Dynamic post-translational modification profiling of *M. tuberculosis*-infected primary macrophages. *Elife* 9:e51461. <https://doi.org/10.7554/eLife.51461>.
67. Cox J, Mann M. 2008. MaxQuant enables high peptide identification rates, individualized p.p.b.-range mass accuracies and proteome-wide protein quantification. *Nat Biotechnol* 26:1367–1372. <https://doi.org/10.1038/nbt.1511>.
68. Jimenez-Morales D, Campos AR, Von Dollen J. 2019. artMS: Analytical R tools for Mass Spectrometry. <https://bioconductor.org/packages/release/bioc/html/artMS.html>. Accessed 2020-02-01.
69. Choi M, Chang CY, Clough T, Broudy D, Killeen T, MacLean B, Vitek O. 2014. MSstats: an R package for statistical analysis of quantitative mass spectrometry-based proteomic experiments. *Bioinformatics* 30:2524–2526. <https://doi.org/10.1093/bioinformatics/btu305>.
70. Perez-Riverol Y, Csordas A, Bai J, Bernal-Llinares M, Hewapathirana S, Kundu DJ, Inuganti A, Griss J, Mayer G, Eisenacher M, Perez E, Uszkoreit J, Pfeuffer J, Sachsenberg T, Yilmaz S, Tiwary S, Cox J, Audain E, Walzer M, Jarnuczak AF, Ternent T, Brazma A, Vizcaino JA. 2019. The PRIDE database and related tools and resources in 2019: improving support for quantification data. *Nucleic Acids Res* 47:D442–D450. <https://doi.org/10.1093/nar/gky1106>.